

Influence of Iron on Phase Stability and Corrosion Resistance of Ti-15%Cr Alloy (Pengaruh Penambahan Besi terhadap Kestabilan Fasa dan Ketahanan Kakisan Alloi Ti-15%Cr)

JUNAIDI SYARIF*, EKO KURNIAWAN, ZAINUDDIN SAJURI & MOHD ZAIDI OMAR

ABSTRACT

In this study, the effect of Fe addition on the phase stability and corrosion resistance of Ti-15%Cr alloys was investigated. The alloying phenomenon in the specimens was also investigated to determine the effectiveness of the application of pure metallic powders as raw materials for the powder metallurgy method. Ti-15%Cr-1%Fe alloys exhibited needle-like structures within equiaxed structures, while Ti-15%Cr-5%Fe and Ti-15%Cr-10%Fe alloys only showed equiaxed grains. XRD results showed that the β phase could be stabilized by the addition of 5% or more Fe to the alloy. Although the pure powders were used as raw materials, the designated chemical composition, i.e. Ti-15%Cr-(1~10)%Fe can be achieved during sintering. The alloying phenomenon occurred upon sintering due to the high diffusivity of Cr and Fe within the β Ti matrix. The corrosion resistance of the newly developed Ti-15%Cr alloys was significantly improved compared with a commercial Ti-6%Al-4%V alloy.

Keywords: Alloying phenomenon; β phase; corrosion resistance; powder metallurgy; sintering

ABSTRAK

Dalam kajian ini, kesan penambahan Fe terhadap kestabilan fasa dan rintangan kakisan pada aloi Ti-15%Cr dikaji. Fenomena pengalioan di dalam spesimen juga telah dikaji untuk menjelaskan keberkesanan penggunaan serbuk logam tulen sebagai bahan mentah untuk kaedah metalurgi serbuk. Alloi Ti-15%Cr-1%Fe mempamerkan struktur seperti jarum di dalam struktur sama paksi. Sebaliknya, aloi Ti-15%Cr-5%Fe dan aloi Ti-15%Cr-10%Fe hanya menunjukkan ira sama paksi sahaja. Hasil XRD menunjukkan bahawa fasa β akan menjadi lebih stabil dengan penambahan Fe lebih besar daripada 5%. Spesimen boleh mencapai komposisi kimia yang ditetapkan iaitu Ti-15% Cr (1 ~ 10)% Fe selepas proses pembuatan dilakukan, meskipun kajian ini menggunakan serbuk logam tulen. Fenomena pengalioan berlaku pada masa persinteran kerana kadar peresapan Cr dan Fe pada matriks β -Ti adalah tinggi. Alloi Ti-15%Cr-Fe juga dikaji dan hasil kajian menunjukkan bahawa ketahanan kakisan aloi tersebut mengalami peningkatan berbanding dengan ketahanan kakisan aloi Ti-6Al-4V yang merupakan aloi komersial.

Kata kunci: Fasa β ; fenomena pengalioan; ketahanan kakisan; metalurgi serbuk; persinteran

INTRODUCTION

The demand for biomaterials has increased significantly in recent years and the number of metallic biomaterials required for hip replacements is predicted to reach 272000 by 2030 (Rack & Qazi 2006). Ti alloys have higher specific strength and better corrosion resistance compared with other alloys or metallic materials and commercially pure (cp) Ti and Ti-6%Al-4%V alloys have been used as metallic orthopedic implant materials. Ti alloys were nominated as the gold standard among metallic implant materials for implantation in soft tissues (Woodman et al. 1984). Unfortunately, cp Ti and Ti-6%Al-4%V alloys still exhibit biomechanical incompatibility due to their relatively high elastic modulus (about 120 GPa). Thus, these materials could cause stress shielding, bone loss and premature failure of the artificial hip (Sumner et al. 1998). Ti-6%Al-4%V alloys can also release toxic ions, such as V and Al ions, into the body, leading to undesirable long-term effects (Nag et al. 2005; Wapner 1991). Many studies have been done on the development

of bcc types of Ti alloy. Since the bcc (β) structure of the Ti system has a lower elastic modulus than the hcp (α) structure, β -type alloys could be designed as new Ti alloys. For instance, β -type Ti-Nb-Ta-Zr alloys have been reported to possess excellent properties required for biomaterials, such as tensile properties, frictional wear properties and low elastic modulus (Niinomi 1998; Taddei et al. 2004; Wei 2011). From viewpoint of *Mo* equivalent, Cr and Fe are strong β -phase stabilizers and can be effective for stabilizing the β phase, as well as Ta and Nb (Lutjering & Williams 2007). Cr and Fe have also been used as alloying elements for commercial metallic biomaterials, such as stainless steel and Co-Cr-Mo alloys. These elements are considered as potential alloying elements for the development of new β Ti alloys from the viewpoint of their biocompatibility with the human body. In this study, the effect of Fe addition on the phase stability and corrosion resistance of Ti-15%Cr alloys was investigated. The alloying phenomenon in the specimen was also investigated to determine the effectiveness of

the application of pure metallic powders as raw materials for the powder metallurgy method.

ALLOY DESIGN AND EXPERIMENTAL PROCEDURES

A molecular orbital method for electronic structures was applied to estimate the β -phase stability of the Ti-15%Cr-Fe alloys (Morinaga et al. 1992). The bond order (Bo) can measure the covalent bond strength between Ti and the other alloying elements, whereas the metal d-orbital energy level (Md) correlates the electronegativity with the metallic radius of the alloying element. Average values of Bo and Md are determined, as shown in the equations below, to predict the stability of the β phase in the Ti-15%Cr-Fe alloys:

$$Bo_{\text{alloy}} = f_{\text{Ti}} Bo_{\text{Ti}} + f_{\text{Cr}} Bo_{\text{Cr}} + f_{\text{Fe}} Bo_{\text{Fe}} \quad (1)$$

$$Md_{\text{alloy}} = f_{\text{Ti}} Md_{\text{Ti}} + f_{\text{Cr}} Md_{\text{Cr}} + f_{\text{Fe}} Md_{\text{Fe}} \quad (2)$$

where f_{Ti} , f_{Cr} , and f_{Fe} are the atomic fractions of Ti, Cr and Fe, respectively. Values of Bo and Md for the elements used in this study are given in Table 1.

TABLE 1. Bo and Md values of each element

Element	Bo	Md
Ti	2.790	2.477
Cr	2.779	1.487
Fe	2.651	0.969

Figure 1 shows a Bo - Md map, in which the areas of α -, α - β - and β -phase alloys are clearly separated (Kuroda 1998; Morinaga 1992). The map also shows the stability of phases as determined by calculations of the average values of Bo and Md . The stability region of β -type alloys has been reported to extend to higher Bo and lower Md regions. Positions of the Ti-15%Cr-Fe alloys are shown in a solid circle plot within the map. Calculations of Bo and Md for different alloys showed that the alloys lie within the region of the β phase. Hence, these alloys can be used as new β -type Ti alloys. In this study, cp Ti, Cr and Fe powders were used as raw materials. The size and purity of the powders are listed in Table 2. The powders were mechanically mixed for 3.6 ks, used to fill in a die cavity (10 mm in diameter) and then compressed under a pressure of 1000 MPa for 3.6 ks using a cold press machine with a capacity of 9 T at ambient temperature. To initiate solid-state bonding between each particle, cylindrical green-compacted samples were sintered at a temperature of 1573 K from 0.6 ks to 14.4 ks and then furnace-cooled under an argon gas atmosphere. Samples were then subjected to solution treatment at 1373 K for 3.6 ks under an argon gas atmosphere, followed by water-quenching. For microstructural observation, specimens were subjected to grinding and polishing until a mirror surface was

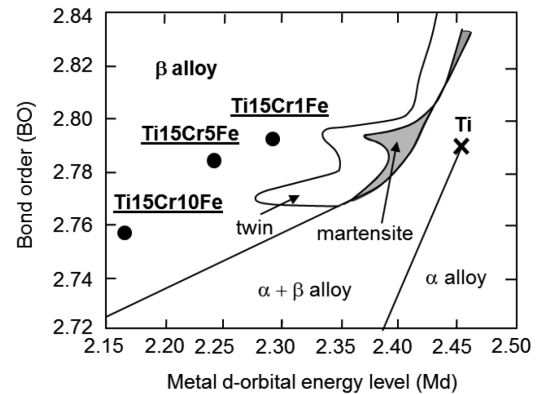


FIGURE 1. A Bo - Md map (Kuroda 1998; Morinaga 1992)

TABLE 2. Size and purity of powder used

Powders	Purity (%)	Size (mesh)
Ti	99	-325
Cr	99	-325
Fe	99	-200

obtained. Then, the specimens were etched by Kroll's solution to reveal microstructure. The microstructure of each specimen was observed by optical microscopy, scanning electron microscopy (SEM) and energy-dispersive X-ray spectroscopy (EDS). The constituent phases of Ti-15%Cr-Fe were identified by X-ray diffractometry (XRD). Specimens were immersed in a 3% NaCl solution and the potential obtained after stabilization during immersion was employed as the open-circuit potential (E_{ocp}) of the alloys. The alloys were anodically and cathodically polarized from the E_{ocp} .

RESULTS AND DISCUSSION

PHASE AND MICROSTRUCTURE OF THE TI-15%CR-Fe ALLOY

Figure 2 shows the optical micrographs of the (a) Ti-15%Cr-1%Fe alloy, (b) Ti-15%Cr-5%Fe alloy and (c) Ti-15%Cr-10%Fe alloy. All samples were subjected to sintering and solution treatment. The Ti-15%Cr-1%Fe alloy exhibited a needle-like structures within an equiaxed structure. Such a structure usually consists of α and β phases. The Ti-15%Cr-5%Fe and Ti-15%Cr-10%Fe alloys showed equiaxed grains. It is indicated that interparticle binding between metallic powders has occurred during sintering although pores were observed within all samples.

Figure 3 shows diffractograms of the alloys. The Ti-15%Cr-1%Fe alloy exhibited a mixture of β phase and hexagonal α phase. XRD diffractograms of the Ti-15%Cr-5%Fe and Ti-15%Cr-10%Fe alloys yielded only the peak for the β phase. Addition of Fe into the alloys to stabilize the β phase was higher than concentration calculated by the Bo - Md calculation in this study: The β

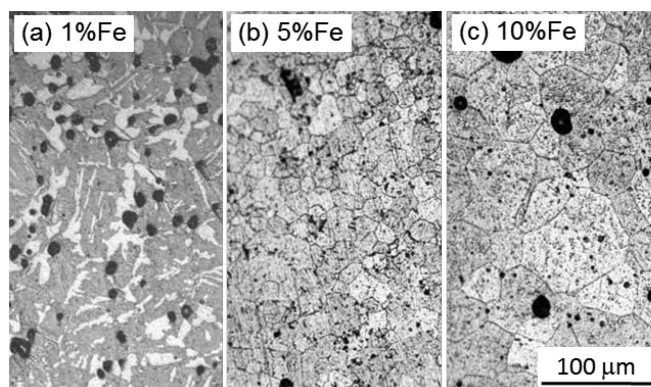


FIGURE 2. Optical micrographs of samples: (a) the Ti-15%Cr-1%Fe alloy, (b) the Ti-15%Cr-5%Fe alloy and (c) the Ti-15%Cr-10%Fe alloy

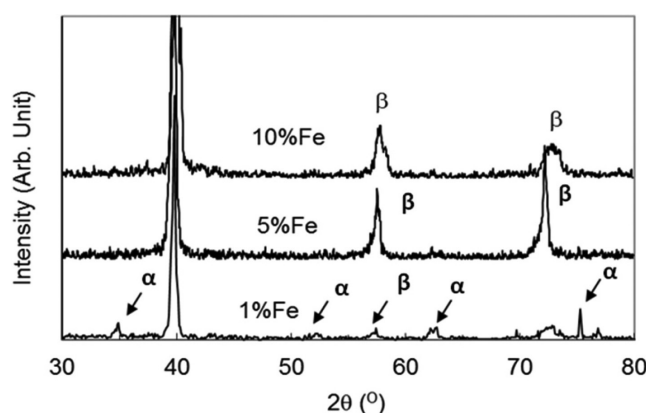


FIGURE 3. XRD diffractograms of the Ti-15%Cr-Fe alloys. The alloys were subjected to sintering and solution treatment

phase will be stabilized at ambient temperature by only 1%Fe addition as shown in Figure 1. Since the powder metallurgy and sintering methods were used in this study, the concentration of impurities in the alloys was believed to be high. Measurement of impurity concentrations using an NOH gas analyzer revealed that the alloys contained high concentrations of oxygen (approximately 0.7 wt. %). An increase in oxygen concentration in the alloy could decrease the stability of its β phase. That is to say, an excess amount of Fe is necessary to stabilize the β phase. The finding obtained in this study is in line with finding reported by Rohmannudin et al. (2009). They have reported that the addition of 10 at. %Fe (10.4 wt. %Fe) can stabilize β phase at ambient temperature in Ti-10 at. %Mo alloy (Rohmannudin et al. 2009).

ALLOYING PHENOMENON DURING SINTERING AND SOLUTION TREATMENT

Since pure metallic powders were used, investigation of the alloying phenomenon in green-compacted samples upon sintering and solution treatment is important. Figure 4 shows SEM micrographs and EDS diffractograms of all samples. Concentrations of elements within the samples were determined by the area mapping mode of EDS from

the SEM micrographs and results of EDS analysis are shown in Table 3. Each element's concentration of the samples that were subjected to sintering and solution treatment reached the designated chemical composition, i.e. Ti-15%Cr-1%Fe, Ti-15%Cr-5%Fe and Ti-15%Cr-10%Fe. Further investigation of the Ti-15%Cr-1%Fe and Ti-15%Cr-5%Fe alloys under higher magnification, as shown in Figure 5 and Table 4, was done to determine the distribution of elements within each phase. Concentrations of elements were analyzed by the point analysis mode of EDS. In the Ti-15%Cr-1%Fe alloy, the black area only showed the presence of Ti, while the white area exhibited the presence of Cr and Fe, the concentrations of which were almost identical to the added concentrations. The black and white areas are believed to be α and β phases, respectively, because β formers, such as Cr and Fe, are enriched at the β phase. The concentrations of elements were nearly identical to the desired chemical composition in the Ti-15%Cr-5%Fe alloy.

The change in concentration of the elements upon sintering was determined to further investigate the alloying phenomenon. The Ti-15%Cr-5%Fe alloy was used as a sample and subjected to sintering for various holding times and quenching. Quenching was done to minimize

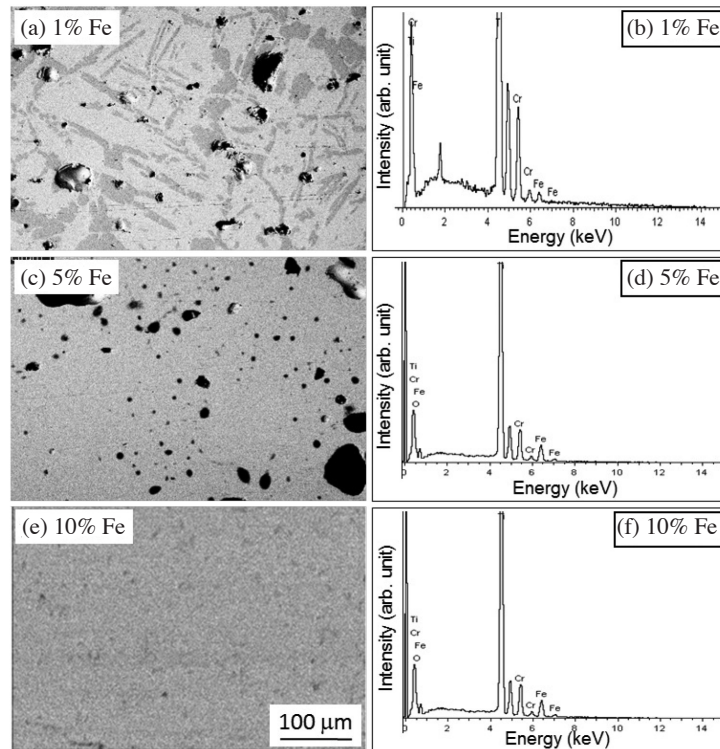


FIGURE 4. SEM micrographs and EDS diffractograms of the microstructures of samples: (a)-(b) the Ti-15%Cr-1%Fe alloy, (c)-(d) the Ti-15%Cr-5%Fe alloy and (e)-(f) the Ti-15%Cr-10%Fe alloy

TABLE 3. Results of area analysis of EDS taken from microstructure shown in Figure 4

	1%Fe	5%Fe	10%Fe
Ti	85.04	81.14	74.41
Cr	13.40	14.25	14.70
Fe	1.56	4.61	10.89

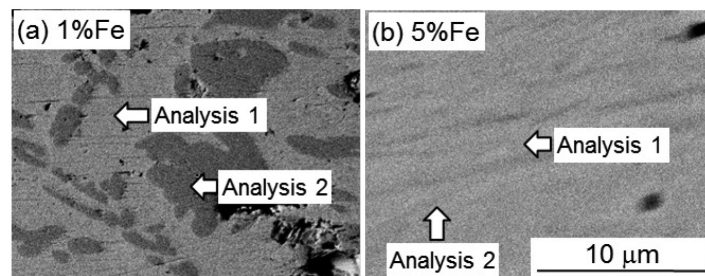


FIGURE 5. SEM micrographs of samples: (a) the Ti-15%Cr-1%Fe alloy and (b) the Ti-15%Cr-5%Fe alloy. Positions where point analysis was done are also represented by arrows

TABLE 4. Results of point analysis by EDS taken from microstructure shown in Figure 5

	T-15%Cr-1%Fe		T-15%Cr-5%Fe	
	Point 1	Point 2	Point 1	Point 2
Ti	99.06	79.39	80.54	80.74
Cr	0.94	19.03	14.81	14.99
Fe	-	1.58	4.65	4.27

the diffusion of elements upon cooling. Figure 6 shows SEM micrographs of the Ti-15%Cr-5%Fe alloys that were sintered at 1300°C for (a) 10 min, (b) 30 min and (c) 90 min. Point analysis by EDS was carried out and the results were summarized in Table 5.

Samples achieved the desired composition after sintering for only 10 min, indicating that alloying occurs upon sintering and solution treatment within a relatively short period of time, likely because of the rapid diffusion of Cr and Fe within the Ti matrix. The diffusivities of Fe and Cr in β Ti have been reported to be over one order of magnitude larger and four times larger than the self-diffusivity of Ti, respectively (Nakajima & Koiwa 1991). Therefore, the designated chemical composition can be achieved by sintering of the green-compacted samples from pure metallic powders.

CORROSION BEHAVIOR

Figure 7 shows the potentiodynamic polarization curves of the Ti-15%Cr-Fe alloys. The potentiodynamic polarization curve of a commercial Ti-6%Al-4%V alloy that was used as a reference is also shown in Figure 7. The corrosion behavior of the Ti-15%Cr-Fe alloys were much better than that of the commercial Ti-6%Al-4%V alloy and the corrosion potential of the experimental alloy improved by Fe addition. The Ti-15%Cr-10%Fe alloy had the highest corrosion potential. Figure 8 shows the corrosion potentials and corrosion rates of the Ti-15%Cr-Fe and Ti-6%Al-4%V alloys. The corrosion potentials and corrosion rates of the Ti-15%Cr-Fe alloys were lower than those of the Ti-6%Al-4%V alloy. Thus, the newly designed Ti-15%Cr-Fe alloys have better corrosion resistance than commercial Ti alloys.

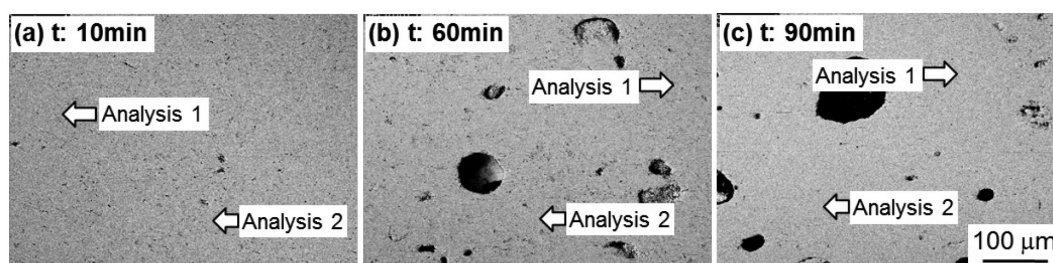


FIGURE 6. SEM micrographs of the Ti-15%Cr-5%Fe alloys. The alloys were sintered at 1300°C for (a) 10 min, (b) 30 min and (c) 90 min

TABLE 5. Results of point analysis of EDS taken from microstructure shown in Figure 6

Point	t = 10 min			t = 60 min			t = 90 min		
	Ti	Cr	Fe	Ti	Cr	Fe	Ti	Cr	Fe
1	81.01	14.57	4.42	80.58	14.43	4.99	80.96	14.04	5.01
2	79.68	14.83	5.49	79.04	15.54	5.42	80.74	14.99	4.27

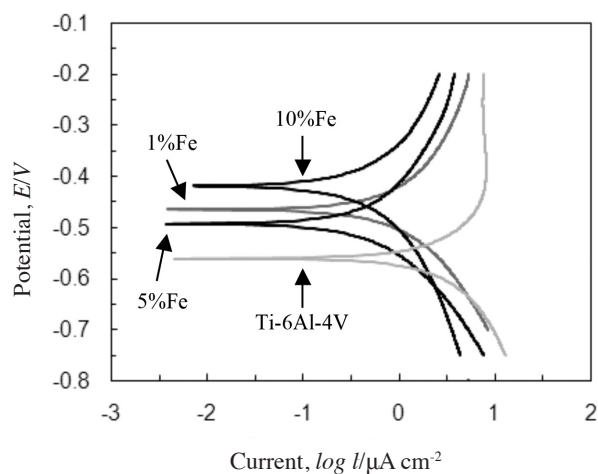


FIGURE 7. Potentiodynamic polarization curves of the Ti-15%Cr-Fe alloys and a commercial Ti-6%Al-4%V alloy as a reference is also shown in the graph

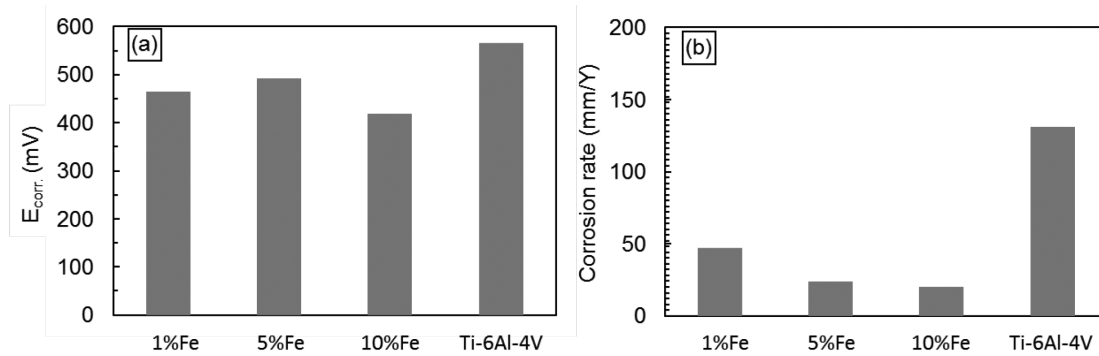


FIGURE 8. Corrosion potential (a) and the corrosion rate (b) of the Ti-15%Cr-Fe alloys and Ti-6Al-4V alloy

CONCLUSION

The influence of Fe on the phase stability and corrosion behavior of Ti-15%Cr alloys was investigated and the following results were obtained. The stability of the β phase increased with increasing Fe concentration. The single β phase can be obtained through the powder metallurgy method for Ti-15%Cr alloys containing 5% or more Fe. The sintering process could enhance interparticle binding and alloying of pure metallic powders to yield the designated chemical composition of the alloy. Addition of Fe improved the corrosion resistance of the Ti-15%Cr alloy.

ACKNOWLEDGEMENTS

The authors would like to thank the Universiti Kebangsaan Malaysia and Ministry of Science, Technology and Innovation (MOSTI), Malaysia for sponsoring this work by Arus Perdana UKM-AP-NBT-14-2010 and Science Fund 03-01-02-SF0263, respectively.

REFERENCES

- Abdel-Hady, M., Hinoshita, K. & Morinaga, M. 2006. General approach to phase stability and elastic properties of b-type Ti-alloys using electronic parameters. *Scripta Mater.* 55: 477-480.
- Kuroda, D., Niinomi, M., Morinaga, M., Kato, Y. & Yashiro, T. 1998. Design and mechanical properties of new β type titanium alloys for implant materials. *Mater. Sci. Eng. A* 243: 244-249.
- Lutjering, G. & Williams, J.C. 2007. *Titanium*. 2nd ed. Berlin: Springer-Verlag.
- Morinaga, M., Kato, M., Kamimura, T., Fukumotom, M., Harada, I. & Kubo, K. 1992. Theoretical design of β -type titanium alloys. *Proceeding of 7th International Conference on Titanium*. pp. 276-283.
- Nag, S., Banerjee, R. & Fraser, H.L. 2005. Microstructural evolution and strengthening mechanisms in Ti-Nb-Zr-Ta, Ti-Mo-Zr-Fe and Ti-15Mo biocompatible alloys. *Mater. Sci. Eng. C* 25: 357-362.
- Nakajima, H. & Koiwa, M. 1991. Diffusion in Titanium. *ISIJ Intl.* 31: 757-766.
- Niinomi, M. 1998. Mechanical properties of biomedical titanium alloys. *Mater. Sci. Eng. A* 243: 231-236.
- Rack, H.J. & Qazi, J.I. 2006. Titanium alloys for biomedical applications. *Mater. Sci. Eng. C* 26: 1269-1277.
- Rohmannudin, T.N., Syarif, J., Omar, M.Z., Sajuri, Z. & Daud, A.R. 2009. Changes in phase stability on Ti-10 at. %Mo Alloy by alloying elements. *International Journal of Mechanical and Materials Engineering* 4: 70-73.
- Sumner, D.R., Turner, T.M., Igloria, R., Urban, R.M. & Galante, J.O. 1998. Functional adaptation and ingrowth of bone vary as a function of hip implant stiffness. *J. Biomech.* 31: 909-917.
- Taddei, E.B., Henriques, V.A.R., Silva, C.R.M. & Cairo, C.A.A. 2004. Production of new titanium alloy for orthopedic implants. *Mater. Sci. Eng. C* 24: 683-687.
- Wapner, K.L. 1991. Implications of metallic corrosion in total knee arthroplasty. *Clin. Orthop. Relat. Res.* 271: 12-20.
- Wei, Q., Wang, L., Fu, Y., Qin, J., Lu, W. & Zhang, D. 2011. Influence of oxygen content on microstructure and mechanical properties of Ti-Nb-Ta-Zr alloy. *Mater. Design* 32: 2934-2939.
- Woodman, J.L., Jacobs, J.J., Galante, J.O. & Urban, R.M. 1984. Metal ion release from titanium-based prosthetic segmental replacements of long bones in baboons long-term study. *J. Orthop. Res.* 1: 421-430.

Department of Mechanical and Materials Engineering
Faculty of Engineering and Built Environment
Universiti Kebangsaan Malaysia
43600 UKM Bangi, Selangor
Malaysia

*Corresponding author; email: syarif@eng.ukm.my

Received: 23 April 2012

Accepted: 26 June 2012